

CONTRIBUTION OF SUPERSTRING Z' BOSON INTO THE POLARIZATION EFFECTS IN PROTON PROTON COLLISIONS

R. Kh. Muradov¹ and A. I. Ahmadov² *

¹ Department of Theoretical Physics, Baku State University,

² High Energy Physics Lab., Faculty of Physics, Baku State University,

Z.Khalilov st. 23, AZ-1148, Baku, Azerbaijan

Abstract

In this work we investigate the single- and the double-spin asymmetries at the collisions of polarized protons $pp \rightarrow (\gamma^*, Z^0, Z') + X$ within the scope of QCD, electroweak interaction and superstring E_6 theory. The helicity amplitude method is used. Analytical expressions for the single- and the double-spin asymmetries are obtained and their dependence from the transverse momentum of lepton pair is investigated at the three different values of invariant masses of lepton pair. Pure contribution coming from superstring Z' boson into the single- and double- spin asymmetries has been extracted. The obtained results allow to investigate the spin structure of the proton.

Keywords: Hadron-hadron collisions; Polarization; Lepton pair production

1 Introduction

With the advent of the RHIC at BNL we have a new facility to study the spin structure of the proton, (for a review on the potential of RHIC [1]), which supplements the existing polarized lepton-hadron machines. Polarized proton-proton collisions with a very high luminosity and a maximum centre of mass energy 500 GeV will provide us with many more details about spin distributions than possible with the existing lepton-hadron machines, which give very little information about the polarized gluon and sea-quark parton densities. The production of lepton pairs in hadron collisions,

*E-mail: ahmadovazar@yahoo.com

the Drell-Yan process [2], is one of the most powerful tools to probe the structure of hadrons. Its parton model interpretation is straightforward—the process is induced by the annihilation of a quark-antiquark pair into a virtual photon which subsequently decays into a lepton pair. The Drell-Yan process in proton-proton or proton-nucleus collisions therefore provides a direct probe of the antiquark densities in protons and nuclei. Since the appearance of the data obtained in the EMC experiment [3], many studies have been devoted to the spin structure of the proton. In the lowest order of perturbative QCD, the spin of the proton can be represented as the sum of three terms; that is,

$$S_p = S_q + S_g + \langle L_z \rangle,$$

where S_q and S_g are, quark and gluon contributions to the proton spin respectively, and $\langle L_z \rangle$ is the contribution of the orbital angular momentum of quarks and gluons.

The experimental results reported in [4-6] suggest that the gluon spin and orbital interaction contribute significantly to the proton spin. Naturally, these experimental results require a theoretical explanation.

Gehrmann [7] calculated $O(\alpha_s)$ correction to x_F and y distributions of dileptons produced in collisions of longitudinally polarized hadrons. He also showed that measurement of the longitudinally polarized cross section for the Drell-Yan process would make it possible to investigate the distribution of polarized sea quarks in hadrons.

In [8], the longitudinal-transverse spin asymmetries (A_{LT}) in Drell-Yan processes were calculated in the leading order for nucleon-nucleon collisions at RHIC energies. It was shown that A_{LT} is much less than the respective transverse-transverse asymmetry A_{TT} .

The Drell-Yan process at high transverse momenta of the dilepton was studied in [9], where the effect of $\gamma - Z^0$ -interference was also taken into consideration. Both single-spin and double-spin asymmetries were investigated there. It was shown that the double-spin asymmetry at small invariant masses of the lepton pair and the single-spin asymmetry at the Z^0 -peak becomes significant.

Also, as it was demonstrated in our work [10] single-spin and double-spin asymmetries in $pp \rightarrow (\gamma^*, Z^0) + X$ processes induced by collisions of polarized hadrons are analyzed on the basis of QCD and electroweak interaction. Here it is shown that the contribution of the Z^0 boson processes into polarized particles, in general, and into the single-spin parity-violating

asymmetries in particular, is significant. The single-spin asymmetries become large, both in the CLW and in the GRSW models, as the dilepton invariant mass approaches the Z^0 - boson mass. Double-spin asymmetry for all the considered p_T is greater than the single-spin asymmetry for all the values of the dilepton invariant mass.

Collisions of polarized hadrons are among processes of greater importance for study of the spin structure of the proton and for calculation of the distributions of polarized quarks in the proton.

The remainder of this paper is organised as follows: in section 2 we shall give some formulae for the amplitudes and the differential cross section for calculations single- and the double-spin asymmetries, in section 3 we present the numerical results and discuss the asymmetries. In Section 4, we draw our conclusions.

In the present paper we investigate contribution superstring Z' boson to the single-spin and double-spin asymmetries in $pp \rightarrow (\gamma^*, Z^0, Z') + X$ processes for studying the spin structure of the proton.

There is currently vigorous research on E_6 theory in elementary particle physics. In the low-energy limit, the E_6 group may be split up into subgroups of fifth or sixth ranks [11]:

$$G_5 = SU_c(3) \times SU_L(2)U_y(1) \times U_\eta(1),$$

$$G_6 = SU_c(3) \times SU_L(2) \times U_y(1) \times U_\psi(1) \times U_\chi(1).$$

One additional neutral vector field Z_η arises in group G_5 , which correspond to $U_\eta(1)$ symmetry. In group G_6 , we have two additional neutral boson fields Z_ψ and Z_χ , which correspond to $U_\psi(1)$ and $U_\chi(1)$ symmetries respectively. A model having the gauge group $SU_c(3) \times SU_L(2) \times U_y(1) \times U(1)$ is now considered as the permissible low-energy limit in superstring theory. An additional Z' boson arises in this model,

$$Z' = Z_\psi \cos \theta_E + Z_\chi \sin \theta_E$$

in which θ_E is the mixing angle ; θ_E is arbitrary for G_6 group, while $\theta_E = 142.24^\circ$ for G_5 . The following is the lagrangian for the interaction of the fundamental fermions with the gauge bosons:

$$L = \frac{e}{2}(J_\mu^\gamma A_\mu + J_\mu^{Z^0} Z_\mu^0 + J_\mu^{Z'} Z'_\mu), \quad (1)$$

in which

$$J_\mu^i = \bar{\Psi}_f \gamma_\mu [g_{L_f}^i (1 + \gamma_s) + g_{R_f} (1 - \gamma_s)] \Psi_f, \quad (2)$$

and $g_{L_f}^i$ and $g_{R_f}^i$ are chiral coupling constants for the fermion f with the gauge bosons $i(i = \gamma, Z^0, Z')$, which eigenvalue are equal:

$$\begin{aligned} g_{L_f}^\gamma &= g_{R_f}^\gamma = Q_f, \quad g_{L_f}^{Z^0} = \frac{2}{\sin 2\Theta_W}(I_3 - Q_f X_W); \\ g_{R_f}^{Z^0} &= \frac{2}{\sin 2\Theta_W}(-Q_f X_W); \\ g_{L_f}^{Z'} &= (5/3)^{0.5} \cdot \frac{1}{\cos \Theta_W}[Q_\psi(f_L) \cos \theta_E + Q_\chi(f_L) \sin \theta_E]; \\ g_{R_f}^{Z'} &= (5/3)^{0.5} \cdot \frac{1}{\cos \Theta_W}[-Q_\psi(f_L) \cos \theta_E + Q_\chi(f_L) \sin \theta_E]; \end{aligned}$$

Here $X_W = \sin^2 \Theta_W$ is the Weinberg parameter, while Q_f and I_{3f} are the generators of $U_\psi(1)$ and $U_\chi(1)$ groups, which correspond to charge and third projection of the isospin for fermion f :

$$\begin{aligned} Q_\psi(f_L) &= \frac{1}{\sqrt{24}}, \quad Q_\chi(f_L) = \frac{3}{\sqrt{40}} \quad \text{for } f_L = (\tilde{d}, e, \nu_e)_L, \\ Q_\psi(f_L) &= \frac{1}{\sqrt{24}}, \quad Q_\chi(f_L) = -\frac{1}{\sqrt{40}} \quad \text{for } f_L = (u, d, \tilde{u}, \tilde{e})_L. \end{aligned}$$

-generators of groups $U_\psi(1)$ and U_χ

The mass matrix for Z^0 and Z' as usual is not diagonalized. This leads to $Z^0 - Z'$ - mixing

$$\begin{pmatrix} Z_1 \\ Z_2 \end{pmatrix} = \begin{pmatrix} \cos \phi & \sin \phi \\ -\sin \phi & \cos \phi \end{pmatrix} \cdot \begin{pmatrix} Z^0 \\ Z' \end{pmatrix}$$

where Z_1 and Z_2 are gauge bosons with physical masses m_{Z_1} and m_{Z_2} , ϕ is an angle mixing, defined by

$$\tan 2\phi = (m_{Z^0}^2 - m_{Z_1}^2)/(m_{Z_2}^2 - m_{Z^0}^2)$$

m_{Z^0} is a mass of Z^0 boson in SM. The expression for Lagrangian interaction fermion with bosons Z_1 and Z_2 obtained from (1) has a form

$$L = \frac{e}{2}(J_\mu^{Z_1} Z_{1\mu} + J_\mu^{Z_2} Z_{2\mu})$$

where currents $J_\mu^{Z_1}$ and $J_\mu^{Z_2}$ have common form (2), but the couplings are defined by

$$g_{L(R)f}^{Z_1} = \cos \phi \cdot g_{L(R)f}^{Z^0} + \sin \phi \cdot g_{L(R)f}^{Z'}$$

$$g_{L(R)f}^{Z_2} = -\sin \phi \cdot g_{L(R)f}^{Z^0} + \cos \phi \cdot g_{L(R)f}^{Z'}$$

This process is performed in the reference frame comoving with the center of mass of primary particles. In order to describe experiments that study the scattering of polarized particles, it is necessary to specify a helicity basis. Here, we use the method of helicity amplitudes. It should be noted that, in [7,8], the asymmetries were studied with allowance for the polarizations of primary particles. Here, we consider asymmetries, taking into account the polarizations of all particles that participate in the reaction under study.

2 Calculation of asymmetry

We begin our analysis by introducing the subprocesses

$$\begin{aligned} g + q &\rightarrow l^+ l^- + q, \\ q + \bar{q} &\rightarrow l^+ l^- + g. \end{aligned} \quad (3)$$

The Feynman diagrams of these subprocess are shown in Fig.1.

The matrix elements for subprocesses (3) with allowance for a virtual photon, Z^0 and Z' - bosons can be represented as

$$\begin{aligned} M_\gamma &= -ie^2 g_s t_{ik}^a \left[\bar{v}(p_4, s_4) \gamma_\mu u(p_3, s_3) \right] \frac{g_{\mu\nu}}{q^2} \bar{u}(p_2, s_2) \hat{\varepsilon} \frac{\hat{f}_1 + m}{f_1^2 - m^2} \gamma_\nu u(p_1, s_1), \\ M_{Z_n} &= -\frac{ig^2 g_s t_{ik}^a}{4 \cos^2 \Theta_W} \sum_{n=1}^{n_Z} \left[\bar{v}(p_4, s_4) \gamma_\mu (L_{e_n} P_L + R_{e_n} P_R) u(p_3, s_3) \right] \times \\ &\quad \times D_{Z_n}(q^2) \bar{u}(p_2, s_2) \hat{\varepsilon} \frac{\hat{f}_1 + m}{f_1^2 - m^2} \gamma_\mu (L_{q_n} P_L + R_{q_n} P_R) u(p_1, s_1); \\ M_\gamma &= -ie^2 g_s t_{ik}^a \left[\bar{v}(p_4, s_4) \gamma_\mu u(p_3, s_3) \right] \frac{g_{\mu\nu}}{q^2} \bar{u}(p_2, s_2) \gamma_\nu \frac{\hat{f}_2 + m}{f_2^2 - m^2} \hat{\varepsilon} u(p_1, s_1), \\ M_{Z_n} &= -\frac{ig^2 g_s t_{ik}^a}{4 \cos^2 \Theta_W} \sum_{n=1}^{n_Z} \left[\bar{v}(p_4, s_4) \gamma_\mu (L_{e_n} P_L + R_{e_n} P_R) u(p_3, s_3) \right] \times \\ &\quad \times D_{Z_n}(q^2) u(p_2, s_2) \gamma_\mu (L_{q_n} P_L + R_{q_n} P_R) \frac{\hat{f}_2 + m}{f_2^2 - m^2} \hat{\varepsilon} u(p_1, s_1); \\ M_\gamma &= -ie^2 g_s t_{ik}^a \left[\bar{v}(p_4, s_4) \gamma_\mu u(p_3, s_3) \right] \frac{g_{\mu\nu}}{q^2} \bar{v}(p_2, s_2) \hat{\varepsilon} \frac{\hat{f}_3 + m}{f_3^2 - m^2} \gamma_\nu u(p_1, s_1), \end{aligned} \quad (4)$$

$$\begin{aligned}
M_{Z_n} &= -\frac{ig^2 g_s t_{ik}^a}{4 \cos^2 \Theta_W} \sum_{n=1}^{n_Z} \left[\bar{v}(p_4, s_4) \gamma_\mu (L_{e_n} P_L + R_{e_n} P_R) u(p_3, s_3) \right] \times \\
&\quad \times D_{Z_n}(q^2) \bar{v}(p_2, s_2) \hat{\varepsilon} \frac{\hat{f}_3 + m}{f_3^2 - m^2} \gamma_\mu (L_{q_n} P_L + R_{q_n} P_R) u(p_1, s_1); \\
M_\gamma &= -ie^2 g_s t_{ik}^a \left[\bar{v}(p_4, s_4) \gamma_\mu u(p_3, s_3) \right] \frac{g_{\mu\nu}}{q^2} v(p_2, s_2) \gamma_\nu \frac{\hat{f}_4 + m}{f_4^2 - m^2} \hat{\varepsilon} u(p_1, s_1), \\
M_{Z_n} &= -\frac{ig^2 g_s t_{ik}^a}{4 \cos^2 \Theta_W} \sum_{n=1}^{n_Z} \left[\bar{v}(p_4, s_4) \gamma_\mu (L_{e_n} P_L + R_{e_n} P_R) u(p_3, s_3) \right] \times \\
&\quad \times D_{Z_n}(q^2) \bar{v}(p_2, s_2) \gamma_\mu (L_{q_n} P_L + R_{q_n} P_R) \frac{\hat{f}_4 + m}{f_4^2 - m^2} \hat{\varepsilon} u(p_1, s_1).
\end{aligned}$$

where $t_{ik}^a = \frac{\lambda_{ik}^a}{2}$ are the Gell-Mann matrices, g_s is the strong-interaction coupling constant,

$$f_1 = p_1 - q, \quad f_2 = p_1 + p_2, \quad f_3 = p_1 - q, \quad f_4 = p_1 - p_5.$$

The helicity amplitudes are denoted by $M(\lambda_1, \lambda_2; \lambda_3, \lambda_4, \lambda_5)$, where λ_1 and λ_2 are helicities of the initial partons, λ_3, λ_4 are the helicities of two leptons, and λ_5 is helicity of the final state parton:

$$M(\lambda_1, \lambda_2; \lambda_3, \lambda_4, \lambda_5) = \begin{cases} M(\lambda_1, \lambda_2; \lambda_3, -\lambda_3, \lambda_2) & \text{for } g + q \rightarrow l^+ l^- + q, \\ M(\lambda_1, -\lambda_1; \lambda_3, -\lambda_3, \lambda_5) & \text{for } q + \bar{q} \rightarrow l^+ l^- + g. \end{cases} \quad (5)$$

Positive- and negative-helicity states are denoted by $|A_\pm\rangle$, they have the following properties:

$$\begin{aligned}
(1 + \gamma_5)|A_\pm\rangle &= 0, \\
|A_+\rangle^c &= -|A_-\rangle, \\
\langle A_\mp | B_\pm \rangle &= -\langle B_\mp | A_\pm \rangle, \\
\langle A_+ | \gamma_\mu | B_+ \rangle &= \langle B_- | \gamma_\mu | A_- \rangle,
\end{aligned} \quad (6)$$

Making use of the Fierz identities we obtain

$$\begin{aligned}
\langle A_+ | \gamma_\mu | B_+ \rangle \langle C_- | \gamma_\mu | D_- \rangle &= 2 \langle A_+ | D_- \rangle \langle C_- | B_+ \rangle, \\
\langle A_- | B_+ \rangle \langle C_- | D_+ \rangle &= \langle A_- | D_+ \rangle \langle C_- | B_+ \rangle + \langle A_- | C_+ \rangle \langle B_- | D_+ \rangle.
\end{aligned} \quad (7)$$

The spinors $u_\pm(p), v_\pm(p)$ describing a particle of momentum p and helicity $\lambda = \pm 1$ satisfy the relations

$$\hat{p}u(p) = \hat{p}v(p) = \bar{u}(p)\hat{p} = \bar{v}(p)\hat{p}, \quad p^2 = 0,$$

$$(1 \pm \gamma_5)v_{\pm} = (1 \mp \gamma_5)u_{\pm} = \bar{u}_{\pm}(1 \pm \gamma_5) = \bar{v}_{\pm}(1 \mp \gamma_5) = 0, \quad (8)$$

$$\bar{u}_{\pm}(p)\gamma_{\mu}u_{\pm}(p) = \bar{v}_{\pm}(p)\gamma_{\mu}v_{\pm}(p) = 2p_{\mu}.$$

Here and below we use the conventional notation

$$\begin{aligned} u_{\pm}(p) &= v_{\mp}(p) = |p_{\pm}\rangle, \\ \bar{u}_{\pm}(p) &= \bar{v}_{\mp}(p) = \langle p_{\pm}|, \\ \langle p_{-}|q_{+}\rangle &= \langle pq\rangle = -\langle qp\rangle, \\ \langle q_{+}|p_{-}\rangle &= \langle pq\rangle^{*} = -\langle qp\rangle^{*}, \\ |\langle pq\rangle|^2 &= 2p \cdot q. \end{aligned} \quad (9)$$

The gluon helicities are defined as follows:

$$\varepsilon_1^{\pm} = \pm \frac{\sqrt{2}}{\langle p_5^{\mp}|p_1^{\pm}\rangle} \left[|p_1^{\mp}\rangle \langle p_5^{\mp}| + |p_5^{\pm}\rangle \langle p_1^{\pm}| \right] \quad \text{for } g + q \rightarrow l^{+}l^{-} + q, \quad (10)$$

$$\varepsilon_5^{\pm} = \pm \frac{\sqrt{2}}{\langle p_1^{\mp}|p_5^{\pm}\rangle} \left[|p_5^{\mp}\rangle \langle p_1^{\pm}| + |p_1^{\pm}\rangle \langle p_5^{\pm}| \right] \quad \text{for } q + \bar{q} \rightarrow l^{+}l^{-} + g. \quad (11)$$

The Mandelstam invariant variables for the subprocess under consideration are defined as

$$\hat{s} = (p_1 + p_2)^2, \quad \hat{t} = (p_5 - p_2)^2 = (Q - p_1)^2, \quad \hat{u} = (p_5 - p_1)^2 = (Q - p_2)^2. \quad (12)$$

Let us consider the reference frame comoving with the center of mass of primary particles, where the momenta of primary hadrons are given by

$$\begin{aligned} P_1 &= \frac{\sqrt{s}}{2}(1, 0, 0, 1), \quad P_2 = \frac{\sqrt{s}}{2}(1, 0, 0, -1), \\ p_1 &= x_1 P_1, \quad p_2 = x_2 P_2, \\ p_5^{\mu} &= p_1^{\mu} + p_2^{\mu} - Q^{\mu}, \\ Q^{\mu} &= p_3^{\mu} + p_4^{\mu}, \\ q^{\mu} &= p_3^{\mu} - p_4^{\mu}; \end{aligned} \quad (13)$$

p_5 is momentum of the outgoing parton. The momenta of two leptons and of the final state parton are taken to be [12]

$$\begin{aligned} p_3^{\mu} &= \frac{1}{2}(E' - q' \cos \alpha, q' \sin \theta - q \sin \alpha \cos \beta \cos \theta - E' \cos \alpha \sin \theta, \\ &\quad -q \sin \alpha \sin \beta, q' \cos \theta - E' \cos \alpha \cos \theta + q \sin \alpha \cos \beta \sin \theta), \end{aligned}$$

$$p_4^\mu = \frac{1}{2}(E' + q' \cos \alpha, q' \sin \theta + q \sin \alpha \cos \beta \cos \theta + E' \cos \alpha \sin \theta, \quad (14)$$

$$q \sin \alpha \sin \beta, q' \cos \theta + E' \cos \alpha \cos \theta - q \sin \alpha \cos \beta \sin \theta),$$

$$p_5 = (q', -q \sin \theta, 0, -q' \cos \theta),$$

where $E' = \frac{\hat{s}+q^2}{2\hat{s}}$ and $q' = \frac{\hat{s}-q^2}{2\hat{s}}$.

We now proceed to computing the square of the matrix element taking into account all helicity states of the particles.

(i) The diagrams in Figs.1.a and 1.b yield

$$\begin{aligned} |M(++; + - +)|^2 &= \left[\sum_{n=1}^{n_z} 2|D_{Z_n}(q^2)|^2 g_s^2 g^4 R_{q_n}^2 L_{e_n}^2 \right. \\ &+ \frac{8g_s^2 e^4 e_q^2}{q^4} + \sum_{\substack{n,n'=1 \\ n < n'}}^{n_z} 4 \cdot \text{Re}[D_{Z_n}(q^2) D_{Z_{n'}}^*(q^2)] g_s^2 g^4 R_{q_n} R_{q_{n'}} L_{e_n} L_{e_{n'}} + \\ &\left. + \sum_{n=1}^{n_z} \frac{[|D_{Z_n}(q^2)|^2 8g_s^2 g^2 e_q R_{q_n} L_{e_n} (q^2 - m_{Z_n}^2)]}{q^2} \right] \times \\ &\times \left\{ \frac{2\pi}{\hat{s}} \hat{t}^2 + \frac{\pi}{\hat{s}} \hat{t} \hat{u} + \pi \hat{u} + 2\pi Q^2 + \frac{\pi}{\hat{s}} \hat{u}^2 + \frac{\pi(Q^2 \hat{t} - \hat{s} \hat{u})}{3\hat{s} \hat{u} (\hat{s} - Q^2)} (\hat{s} \hat{t} \hat{u} + Q^2 \hat{s} \hat{t} - \hat{s}^2 \hat{u} - \hat{s} \hat{u}^2 - \right. \\ &\left. - Q^2 \hat{u} \hat{t} - Q^2 \hat{t}^2) + \frac{4\pi Q^2 (\hat{t}^2 + \hat{u} \hat{t} - \hat{s} \hat{t})}{3(\hat{s}^2 - Q^2)} \right\}, \quad (15) \end{aligned}$$

$$|M(++; - + +)|^2 = |M(++; + - +)|^2,$$

$$\begin{aligned} |M(+ - ; + - -)|^2 &= \left[\sum_{n=1}^{n_z} 2|D_{Z_n}(q^2)|^2 g_s^2 g^4 L_{q_n}^2 L_{e_n}^2 + \frac{8g_s^2 e^4 e_q^2}{q^4} + \right. \\ &+ \sum_{\substack{n,n'=1 \\ n < n'}}^{n_z} 4 \text{Re}[D_{Z_n}(q^2) D_{Z_{n'}}^*(q^2)] g_s^2 g^4 L_{q_n} L_{q_{n'}} L_{e_n} L_{e_{n'}} + \\ &\left. + \sum_{n=1}^{n_z} \frac{[|D_{Z_n}(q^2)|^2 8g_s^2 g^2 e_q L_{q_n} L_{e_n} (q^2 - m_{Z_n}^2)]}{q^2} \right] \\ &\times \left\{ \frac{-\pi Q^2}{\hat{s} \hat{u}} (\hat{t} + \hat{u} + 2Q^2)^2 - \frac{\pi Q^2}{3\hat{s} \hat{u} (\hat{s} - Q^2)^2} (Q^2 \hat{t} + Q^2 \hat{u} - \hat{s} \hat{t} - \hat{s} \hat{u})^2 \right\} \quad (16) \end{aligned}$$

$$|M(+ - ; - + -)|^2 = |M(+ - ; + - -)|^2 \quad \text{for } R_e \longleftrightarrow L_e.$$

(ii) The contribution of the diagrams in Figs.1.c and 1.d is

$$|M(+ - ; + - +)|^2 = \left[\sum_{n=1}^{n_z} 2|D_{Z_n}(q^2)|^2 g_s^2 g^4 L_{q_n}^2 L_{e_n}^2 + \frac{8g_s^2 e^4 e_q^2}{q^4} + \right.$$

$$\begin{aligned}
& \sum_{\substack{n, n'=1 \\ n < n'}}^{n_Z} 4 \cdot \text{Re}[D_{Z_n}(q^2) D_{Z_{n'}}^*(q^2)] g_s^2 g^4 L_{q_n} L_{q_{n'}} L_{e_n} L_{e_{n'}} + \\
& + \sum_{n=1}^{n_Z} \left[\frac{|D_{Z_n}(q^2)|^2 8 g_s^2 g^2 e_q L_{q_n} L_{e_n} (q^2 - m_{Z_n}^2)}{q^2} \right] \times \\
& \times \left\{ \pi Q^2 \frac{\hat{t}}{\hat{u}} + \frac{\pi Q^2 (Q^2 \hat{u} - \hat{s} \hat{t})^2}{3 \hat{u} \hat{t} (\hat{s} - Q^2)^2} + \frac{4\pi}{3} \frac{Q^4 \hat{s}}{(\hat{s} - Q^2)^2} \right\}, \tag{17}
\end{aligned}$$

$$|M(+--; -++)|^2 = |M(+--; +-+)|^2 \quad \text{for} \quad R_e \longleftrightarrow L_e,$$

$$\begin{aligned}
|M(+--; +- -)|^2 &= \left[\sum_{n=1}^{n_Z} 2 |D_{Z_n}(q^2)|^2 g_s^2 g^4 L_{q_n}^2 L_{e_n}^2 + \frac{8 g_s^2 e^4 e_q^2}{q^4} + \right. \\
& + \sum_{\substack{n, n'=1 \\ n < n'}}^{n_Z} 4 \cdot \text{Re}[D_{Z_n}(q^2) D_{Z_{n'}}^*(q^2)] g_s^2 g^4 L_{q_n} L_{q_{n'}} L_{e_n} L_{e_{n'}} + \\
& + \sum_{n=1}^{n_Z} \left[\frac{|D_{Z_n}(q^2)|^2 8 g_s^2 g^2 e_q L_{q_n} L_{e_n} (q^2 - m_{Z_n}^2)}{q^2} \right] \times \\
& \times \left\{ \frac{2\pi}{3} \frac{(Q^2 \hat{t} - \hat{s} \hat{u})^2}{\hat{u} (\hat{s} - Q^2)^2} + \frac{\pi \hat{s} (Q^2 \hat{t} - \hat{u} \hat{s})^2}{3 \hat{u} \hat{t} (\hat{s} - Q^2)^2} + \frac{4\pi}{3} \frac{Q^2 \hat{s} \hat{t}}{(\hat{s} - Q^2)^2} + \right. \\
& + \left. \frac{4\pi}{3} \frac{Q^2 \hat{s}^2}{(\hat{s} - Q^2)^2} - 2\pi \hat{u} - 2\pi Q^2 - \pi \frac{\hat{s} \hat{u}}{\hat{t}} - 2\pi Q^2 \frac{\hat{s}}{\hat{t}} \right\}, \tag{18}
\end{aligned}$$

$$|M(+--; -+-)|^2 = |M(+--; +- -)|^2 \quad \text{for} \quad R_e \longleftrightarrow L_e.$$

The following abbreviation have been used

$$D_{Z_n}(q^2) = \frac{1}{q^2 - m_{Z_n}^2 + i m_{Z_n} \Gamma_{Z_n}}.$$

For $n_Z = 1$ one recovers the cross section of the MSSM [10]. In models $R5_1$ and $R5_2$ the number of neutral gauge bosons is $n_Z=2$, in models $R6$ $n_Z=3$. Note that all couplings are assumed to be real due to CP conservation.

The experimental lower mass bounds on the new E_6 gauge bosons are about 600 GeV [14]. For calculation we assume $m_{Z_2} = 1264$ GeV in the model $R5_1$, $m_{Z_2} = 1786$ GeV in $R5_2$ and $m_{Z_3} = 1786$ GeV in $R6$. The widths of the new gauge bosons are estimated by $\Gamma_{Z_{2,3}} = 0.014 m_{Z_{2,3}}$ [15]. All scalar products $p_i \cdot p_j$ can be expressed in terms of Mandelstam variables [13]:

$$s_{12} = \hat{s},$$

$$\begin{aligned}
s_{13} &= 2p_1p_3 = \frac{1}{2}(Q^2 - \hat{t}) - \frac{Q^2\hat{u} - \hat{s}\hat{t}}{2(\hat{s} - Q^2)} \cos \alpha - \frac{\sqrt{Q^2\hat{s}\hat{t}\hat{u}}}{\hat{s} - Q^2} \sin \alpha \cos \beta, \\
s_{14} &= 2p_1p_4 = \frac{1}{2}(Q^2 - \hat{t}) + \frac{Q^2\hat{u} - \hat{s}\hat{t}}{2(\hat{s} - Q^2)} \cos \alpha + \frac{\sqrt{Q^2\hat{s}\hat{t}\hat{u}}}{\hat{s} - Q^2} \sin \alpha \cos \beta, \\
s_{15} &= 2p_1p_5 = -\hat{u} \\
s_{23} &= 2p_2p_3 = \frac{1}{2}(Q^2 - \hat{u}) - \frac{Q^2\hat{t} - \hat{s}\hat{u}}{2(\hat{s} - Q^2)} \cos \alpha + \frac{\sqrt{Q^2\hat{s}\hat{t}\hat{u}}}{\hat{s} - Q^2} \sin \alpha \cos \beta, \quad (19) \\
s_{24} &= 2p_2p_4 = \frac{1}{2}(Q^2 - \hat{u}) + \frac{Q^2\hat{t} - \hat{s}\hat{u}}{2(\hat{s} - Q^2)} \cos \alpha - \frac{\sqrt{Q^2\hat{s}\hat{t}\hat{u}}}{\hat{s} - Q^2} \sin \alpha \cos \beta, \\
s_{25} &= 2p_2p_5 = -\hat{t}, \\
s_{34} &= 2p_3p_4 = Q^2, \\
s_{35} &= 2p_3p_5 = -\frac{\hat{u} + \hat{t}}{2}(1 - \cos \alpha), \\
s_{45} &= 2p_4p_5 = -\frac{\hat{u} + \hat{t}}{2}(1 + \cos \alpha).
\end{aligned}$$

Integration over the final states in phase space can be simplified by employing the relation

$$\frac{1}{(2\pi)^9} \frac{d^3p_3}{2E_3} \frac{d^3p_4}{2E_4} \frac{d^3p_5}{2E_5} \delta(p_1 + p_2 - q - p_5) = \frac{1}{(2\pi)^9} \frac{1}{16} d\Omega \pi \delta(\hat{s} + \hat{t} + \hat{u} - Q^2) \frac{dQ^2 d\hat{t} d\hat{u}}{\hat{s}}. \quad (20)$$

The effective cross section for $pp \rightarrow l^+l^- + X$ processes can be represented in the form [16]

$$\begin{aligned}
E \frac{d\sigma}{dQ^2 d^3p} &= \int_{x_1^{\min}}^1 \int_{x_2^{\min}}^1 dx_1 dx_2 G^A(x_1) G^B(x_2) \frac{\hat{s}}{\pi} \frac{d\hat{\sigma}}{dQ^2 d\hat{t} d\hat{u}} \delta(\hat{s} + \hat{t} + \hat{u} - Q^2), \quad (21) \\
\pi E \frac{d\sigma}{d^3p} &= \frac{d\sigma}{dy dp_T^2}.
\end{aligned}$$

where y is the rapidity of the lepton pair, p_T is its transverse momentum, and $G^A(x_1)$ and $G^B(x_2)$ are distributions of the partons in the proton. From expression (21), it follows that, in the double-spin case, the correlation effective cross section has a form

$$\frac{d\Delta\sigma}{dQ^2 dy dp_T^2} = \int_{x_1^{\min}}^1 \int_{x_2^{\min}}^1 dx_1 dx_2 \Delta G^A(x_1) \Delta G^B(x_2) \hat{s} \frac{d\Delta\hat{\sigma}}{dQ^2 d\hat{t} d\hat{u}} \delta(\hat{s} + \hat{t} + \hat{u} - Q^2), \quad (22)$$

$$d\Delta\sigma = \frac{1}{2}(d\sigma^{(++)} - d\sigma^{(+-)}),$$

whereas, in the single-spin case, we obtain

$$\frac{d\Delta\sigma}{dQ^2 dy dp_T^2} = \int_{x_1^{min}}^1 \int_{x_2^{min}}^1 dx_1 dx_2 \Delta G^A(x_1) G^B(x_2) \hat{s} \frac{d\Delta\hat{\sigma}}{dQ^2 d\hat{t} d\hat{u}} \delta(\hat{s} + \hat{t} + \hat{u} - Q^2), \quad (23)$$

$$\begin{aligned} d\Delta\sigma &= d\sigma^{(+)} - d\sigma^{(-)} = \frac{1}{2}(d\sigma^{(++)} + d\sigma^{(+-)} - d\sigma^{(-+)} - d\sigma^{(--)}), \\ \hat{s} &= x_1 x_2 s, \\ \hat{t} &= x_1 t + (1 - x_1) Q^2, \\ \hat{u} &= x_2 u + (1 - x_2) Q^2, \\ t &= Q^2 - m_T \sqrt{s} e^{-y}, \\ u &= Q^2 - m_T \sqrt{s} e^y \end{aligned} \quad (24)$$

where Q^2 is the invariant mass of the lepton pair and m_T – is the transverse mass, which is given by

$$\begin{aligned} m_T^2 &= Q^2 + p_T^2; \\ x_1 &= \frac{x_2 \sqrt{s} \sqrt{Q^2 + p_T^2} e^y - Q^2}{x_2 s - \sqrt{s} \sqrt{Q^2 + p_T^2} e^{-y}}; \quad x_2 = \frac{x_1 \sqrt{s} \sqrt{Q^2 + p_T^2} e^{-y} - Q^2}{x_1 s - \sqrt{s} \sqrt{Q^2 + p_T^2} e^y}; \end{aligned} \quad (25)$$

$$\begin{aligned} x_1^{min} &= \frac{-u}{s + t - Q^2} = \frac{\sqrt{s} \sqrt{Q^2 + p_T^2} e^y - Q^2}{s - \sqrt{s} \sqrt{Q^2 + p_T^2} e^{-y}}; \\ x_2^{min} &= \frac{-t}{s + t - Q^2} = \frac{\sqrt{s} \sqrt{Q^2 + p_T^2} e^{-y} - Q^2}{s - \sqrt{s} \sqrt{Q^2 + p_T^2} e^y}. \end{aligned} \quad (26)$$

In order to compute single- and the double-spin asymmetries, we introduce the quantities

$$\begin{aligned} d\hat{\sigma}^{(++)} \pm d\hat{\sigma}^{(+-)} &\sim \left\{ (|M(++;+-+)|^2 + |M(++;-++)|^2 \pm |M(+--;+-+)|^2 \pm \right. \\ &\quad \pm |M(+--;-+-)|^2) \pm (|M(+--;+-+)|^2 + |M(+--;-++)|^2 + \\ &\quad \left. + |M(+--;+-+)|^2 + |M(+--;-+-)|^2 \right\}, \end{aligned} \quad (27)$$

$$\begin{aligned} d\hat{\sigma}^{(+)} \pm d\hat{\sigma}^{(-)} &\sim \left\{ (|M(++;+-+)|^2 + |M(++;-++)|^2 + |M(+--;+-+)|^2 + \right. \\ &\quad + |M(+--;-+-)|^2 \pm |M(-+;+-+)|^2 \pm |M(-+;-++)|^2 \pm |M(--;+-+)|^2 \pm \\ &\quad \left. \pm |M(--;-+-)|^2) + (|M(+--;+-+)|^2 + |M(+--;-++)|^2 + \right. \end{aligned}$$

$$+|M(+--; -++)|^2 + |M(+--; -+-)|^2 \pm |M(-++; +- -)|^2 \pm \\ \pm |M(-++; + - +)|^2 \pm |M(-++; -++)|^2 \pm |M(-++; -+-)|^2 \Big\}, \quad (28)$$

For this purpose, we also use the well-known expressions

$$A_L = \frac{\frac{d\sigma^{(+)}}{dQ^2 dy dp_T^2} - \frac{d\sigma^{(-)}}{dQ^2 dy dp_T^2}}{\frac{d\sigma^{(+)}}{dQ^2 dy dp_T^2} + \frac{d\sigma^{(-)}}{dQ^2 dy dp_T^2}}, \quad (29)$$

$$A_{LL} = \frac{\frac{d\sigma^{(++)}}{dQ^2 dy dp_T^2} - \frac{d\sigma^{(+-)}}{dQ^2 dy dp_T^2}}{\frac{d\sigma^{(++)}}{dQ^2 dy dp_T^2} + \frac{d\sigma^{(+-)}}{dQ^2 dy dp_T^2}}. \quad (30)$$

3 Numerical results and discussion

In order to compute single- and the double-spin asymmetries numerically, we employ two functions that describe the distribution of polarized quarks which were proposed by Cheng et al. [17] (the CLW model) and by Gluck et al. [18] (the GRSV model). We use two sets of parameters for each function. For unpolarized quarks the distribution function was found by Martin et al.[19].

In this paper we have studied the dependences of the single- A_L and the double-spin A_{LL} asymmetries on the dilepton transverse momentum at RHIC energies ($\sqrt{s} = 500$ GeV) for various values of the dilepton invariant mass: $Q = 10$ GeV, 60 GeV and $Q = m_{Z^0}$.

The single-spin asymmetry in $pp \rightarrow l^+l^- + X$ processes as a function of the transverse momentum of the lepton pair is shown in Figs.2-4 at $\sqrt{s} = 500$ GeV for three values of the dilepton invariant mass. The single-spin asymmetry A_L as a function of the dilepton transverse momentum p_T is presented Fig.2 at the dilepton invariant mass of $Q = 10$ GeV and the rapidity of $y = 0$. As it is seen for the single-spin asymmetry A_L , the result within the CLW model differs a little from that within the GRSV model. Also, as it is seen from Figs.2-4 the dependence of the single-spin asymmetry A_L on the dilepton transverse momentum demonstrates the same behavior. Single-spin asymmetry is monotonously increase with increase of the dilepton transverse momentum. As the dilepton invariant mass varies from $Q = 10$ GeV to $Q = m_{Z^0}$, the single-spin asymmetry can take either positive or negative values. At the dilepton invariant mass $Q = 10$ GeV for the single-spin asymmetry A_L , the result within the CLW model differs from that within the GRSV model and is equal to 2.4 percent.

Also, at the dilepton invariant mass $Q = 60\text{GeV}$ and m_{Z^0} for single-spin asymmetries differs between CLW and GRSV model approximately 3 and 4 percent. It should be noted that, over the entire invariant-mass range under consideration, the single-spin asymmetries in the GRSV model are almost independent of the choice of the set of partons' distribution amplitudes.

The double-spin asymmetry in $pp \rightarrow l^+l^- + X$ processes as a function of the dilepton transverse momentum at the rapidity of $y = 0$ and the energy of $\sqrt{s} = 500 \text{ GeV}$ is illustrated in Figs.5-7 for three values of the dilepton invariant mass: $Q = 10 \text{ GeV}$, 60 GeV , m_{Z^0} and the rapidity of $y = 0$. For all values of the dilepton invariant mass, the double-spin asymmetry is greater than the single-spin asymmetry for p_T values considered in these figures. As it is seen from Figs.5-7 the dependence of the double-spin asymmetry A_{LL} on the dilepton transverse momentum demonstrates the same behavior. Double-spin asymmetry is monotonously decreasing with increase of the dilepton transverse momentum. At the dilepton invariant mass $Q = 10 \text{ GeV}$, 60 GeV and m_{Z^0} for double-spin asymmetries differs between CLW and GRSV models approximately 7; 5 and 4 percent, respectively.

The Figs.8-9 show contribution of Z' boson into the single-and the double-spin asymmetries as the function of the dilepton transverse momentum at the value of the dilepton invariant mass $Q = m_{Z^0}$ (single-spin asymmetry), 10 GeV (double-spin asymmetry).

In the present work we performed numerical analysis of single-and double-spin asymmetries for $pp \rightarrow (\gamma^*, Z^0, Z') + X$ processes using the method of helicity amplitudes. Asymmetries were explored in the domain of high momentum transfers at RHIC energies. We employed the distributions of polarized partons within CLW [17] and GRSV [18] models. Both the CLW and the GRSV functions were obtained in the second order of perturbation theory. The distribution of unpolarized partons was taken from [19]. In general, the distinction between the single-spin asymmetries A_L for the two sets of partons in CLW model is greater than that in GRSV model. These asymmetries generally increase as the dilepton mass approaches the Z^0 -boson mass. The distinction between the two sets in GRSV model is small. However, as the transverse momentum p_T , varies within the range $\sim 10 \div 110 \text{ GeV}/c$, the double-spin asymmetries A_{LL} are of the same order of magnitude at the three values of Q . At various values of p_T , the difference between the asymmetries for the two sets of partons in CLW model is greater than that in GRSV model. The difference of the asymmetries for

the two sets in GRSV model is nearly constant.

The contribution of the Z^0 and Z' - bosons processes into polarized particles, in general, and to the single-spin parity-violating asymmetries, in particular, is significant. The single-spin asymmetries become large, both in CLW and in GRSV models, as the dilepton invariant mass approaches the Z^0 - boson mass. Over the range of p_T under study, the double-spin asymmetry is greater than the single-spin asymmetry for all values of the dilepton mass.

Analysis shows that with increase of mass of superstring Z' boson character dependence asymmetries on the tranverse momentum of lepton pair is not changed. Also, we compared this calculation with [10]. Analysis shows that at the value of dilepton invariant masses $Q = 10 \text{ GeV}$, 60 GeV , m_{Z^0} contribution coming from Z' boson on the single-and the double - spin asymmetries is considerable. Contribution of superstring Z' boson is evident in the interference term. Also pure contribution coming from superstring Z' boson into the single-and the double-spin asymmetries has been extracted. It is shown that with increase of mass of this boson to the single-and the double-spin asymmetries increase. In general, we can show that single-and the double-spin asymmetries have the form:

$$A_{L(LL)} = A_{L(LL)}^{\gamma, Z^0} + \Delta A_{L(LL)}$$

where $\Delta A_{L(LL)}$ consist of interference term between superstring Z' boson with Z^0 and γ boson and contribution coming from superstring Z' boson, with lepton pair production from Z' boson. Our calculation shows that contribution of $\Delta A_{L(LL)}$ into single-spin asymmetries at the value of dilepton invariant masses $Q = 10 \text{ GeV}$, 60 GeV , m_{Z^0} is about $7.1 \div 10$, $16.9 \div 19.9$, $19.4 \div 23.3$ and to the double -spin asymmetries is about $23.3 \div 28.8$, $22.8 \div 26.8$, $16.9 \div 20.9$ percent depending on transverse momentum of the lepton pair respectively. Both the single-spin and the double-spin asymmetries are sensitive to the polarised gluon distribution and may be used as probes of the spin structure of the proton

4 Conclusions

In this paper we have studied both the single-and the double-spin asymmetries of the transverse momentum lepton pairs at RHIC energies ($\sqrt{s} = 500 \text{ GeV}$). At these high energies, Z^0 can contribute significantly into the Drell-Yan process, inducing a parity -violating single-spin asymmetry.

This asymmetry may be measured in experiments where only one of the initial particles is polarized. Using these angular distributions, we have constructed single-and double-spin asymmetries, which we then studied numerically using four sets, which both sets (CLW and GRSV) were obtained in the second order of perturbation theory. We have found that the single-spin asymmetries are measurably large only at large dilepton masses, i.e. close to the Z^0 peak. The double-spin asymmetries are large even at smaller dilepton masses. Both the single-spin and double-spin asymmetries are sensitive to the polarized gluon distribution and may be used as probes of the spin structure of the proton. As it is shown on figures with increase of mass of superstring Z' boson character dependence asymmetries on the transverse momentum of lepton pair is not changed. Analysis shows that at the value of dilepton invariant masses $Q = 10 \text{ GeV}, 60 \text{ GeV}, m_{Z^0}$ contribution coming from Z' boson into the single-and the double-spin asymmetries is considerable. Contribution of superstring Z' boson is evident in the interference term. Also, pure contribution coming from superstring Z' boson on the single-and double-spin asymmetries has been extracted. It is shown that with increase of mass of this boson the single-and the double-spin asymmetries increase. Our calculation shows that contribution of $\Delta A_{L(LL)}$ into single-spin asymmetries at the value of dilepton invariant masses $Q = 10 \text{ GeV}, 60 \text{ GeV}, m_{Z^0}$ is about $7.1 \div 10, 16.9 \div 19.9, 19.4 \div 23.3$ and to the double -spin asymmetries is about $23.3 \div 28.8, 22.8 \div 26.8, 16.9 \div 20.9$ percent depending on transverse momentum of the lepton pair respectively.

Therefore, measurement of the single-and the double-spin asymmetry helps in study of the spin structure of the proton.

Acknowledgment

One of us Dr. A. Ahmadv grateful to NATO Reintegration Grant-980779.

References

- [1] G. Bunce, N.Saito, J.Soffer, W.Vogelsang, Annu.Rev.Nucl.Part.Sci. 50, 525 (2000).
- [2] S. D.Drell, T.M.Yan, Phys. Rev. Lett. 25, 316 (1970).
- [3] EMC Collab.(J. Ashman et al.), Phys. Lett. B206, 364 (1988).
- [4] K. Abe et al., Phys.Rev.Lett. 74, 346 (1995).
- [5] D. L. Anthony et al., Phys.Rev.Lett. 71, 959 (1993).
- [6] D. Adams et al., Phys.Lett. B357, 248 (1995).
- [7] T. Gehrmann, Nucl.Phys. B498, 245 (1997).
- [8] Y. Kanazawa, Y. Koike, N. Nishiyama, Phys.Lett. B430, 195 (1998)
- [9] E. Leader, K. Sridhar, Phys.Lett. B311, 324 (1993).
- [10] R. Kh. Muradov, A. I. Akhmedov and R. M. Burdjaliev, Physics of Atomic Nuclei, V65, N7, 1352 (2002)
- [11] M. B. Green, J. H. Schwars, Phys.Lett. B149, 117 (1984)
- [12] R. D. Carlits, R. S. Willey, Phys.Rev. D45, 2323 (1992).
- [13] E. Byckling and K. Kajantie, Particle Kinematics. (Wiley, New York, 1973; Mir, Moscow, 1975).
- [14] F. Abe et.al.(CDF Collaboration), Phys.Rev. D50, 6734 (1994).
- [15] T. Gherghetta, T. A. Kaeding and G. L. Kane, Phys.Rev. D57, 3178 (1998).
- [16] E. Reya, Phys.Rep. 69, 292 (1981).
- [17] H.- Y. Cheng, H. H. Liu, C.- Y. Wu, Phys.Rev. D53, 2380 (1996).
- [18] M. Gluck, E. Reya, M. Stratmann, W. Vogelsang, Phys.Rev. D53, 4775 (1996).
- [19] A. D. Martin, R. G. Roberts, W. J. Stirling, Phys.Rev. D50, 6734 (1994).

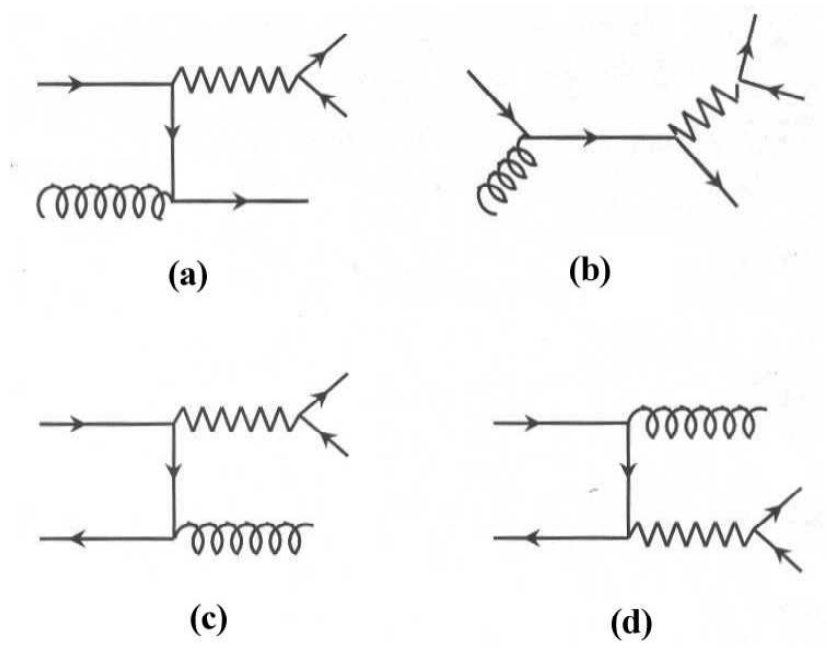


Figure 1: Parton-level subprocesses contributing into the Drell-Yan process: (a),(b)-quark-gluon Compton scattering; (c),(d)-real gluon corrections to $q\bar{q}$ annihilation.

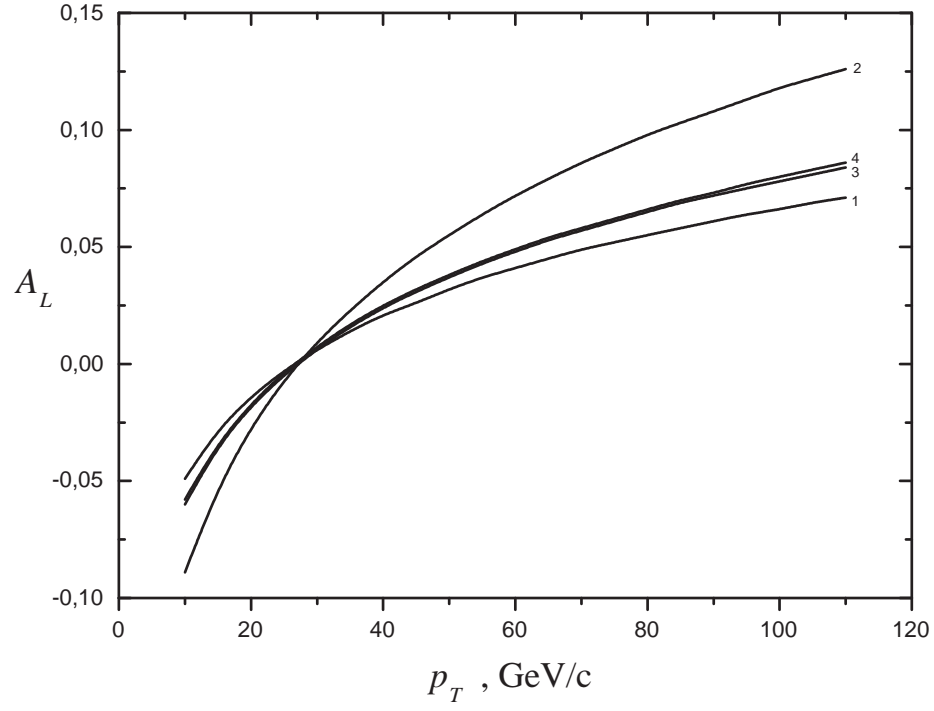


Figure 2: Single-spin asymmetry in $pp \rightarrow l^+l^- + X$ processes as a function of the dilepton transverse momentum at $\sqrt{s} = 500$ GeV, the dilepton invariant mass of $Q = 10$ GeV, and the rapidity of $y = 0$. Shown in the figure are the results obtained on the basis of the CLW model with set I (curve 1) and set II (curve 2) and on the basis GRSV model with set I (curve 3) and set II (curve 4).

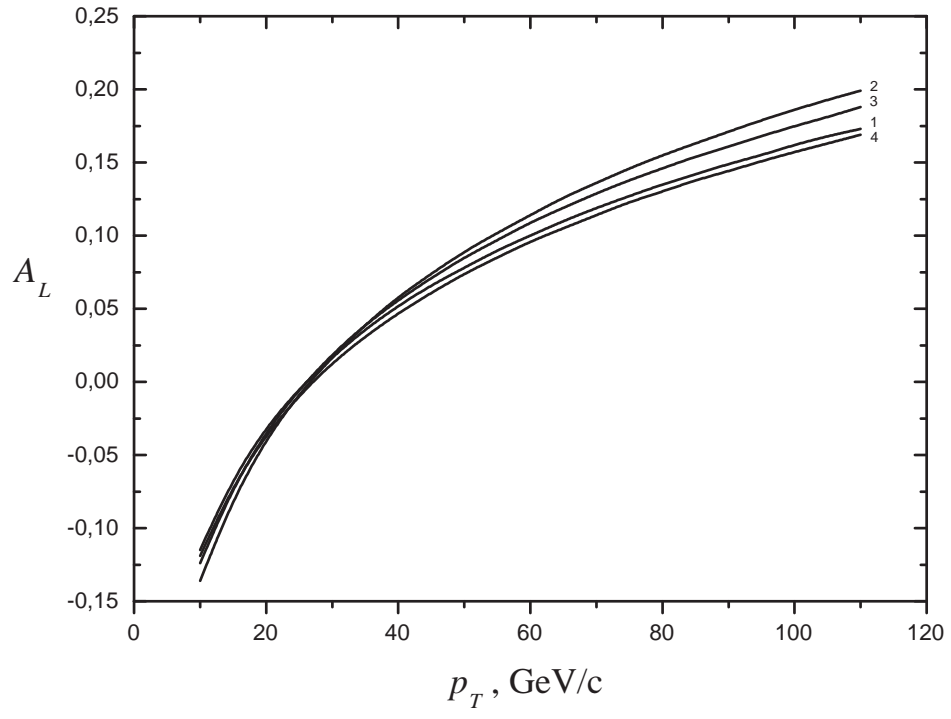


Figure 3: As in Fig.2, but for $Q = 60$ GeV.

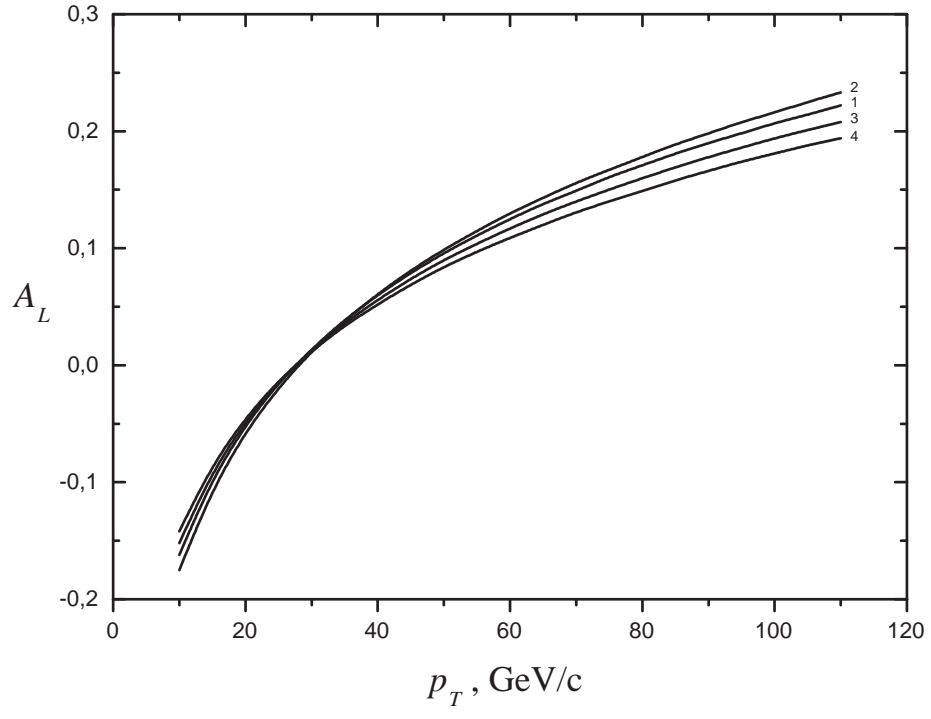


Figure 4: As in Fig.2, but for $Q = m_{Z^0}$.

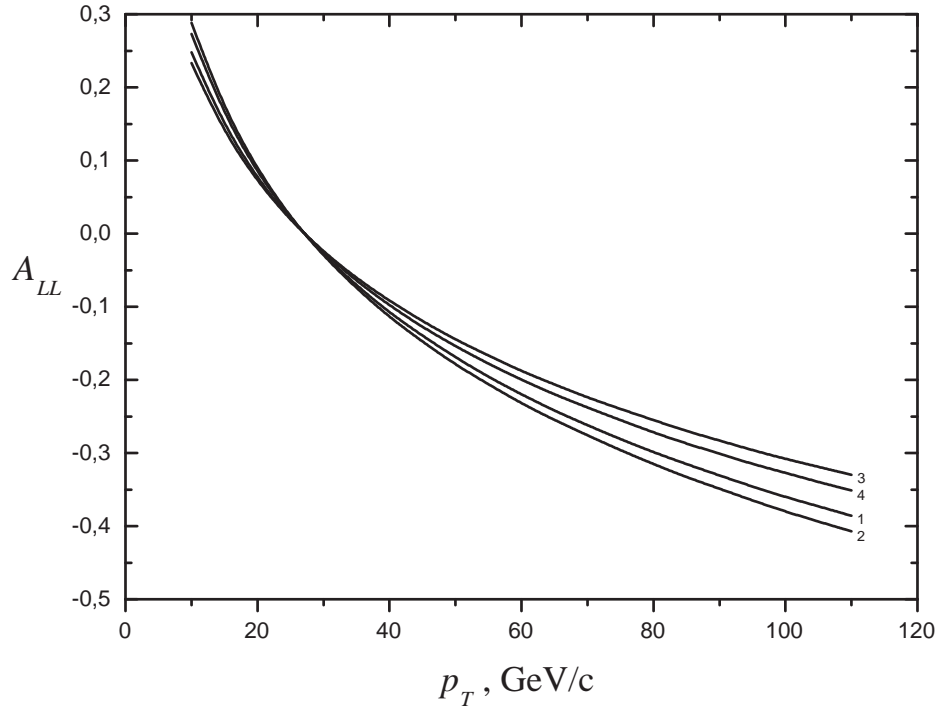


Figure 5: Double-spin asymmetry $pp \rightarrow l^+l^- + X$ in the processes as a function of the dilepton transverse momentum at $\sqrt{s} = 500$ GeV, the dilepton invariant mass of $Q = 10$ GeV, and the rapidity of $y = 0$. Shown are the asymmetries obtained on the basis of the CLW model with (curve 1) set I and (curve 2) set II and on the basis of the GRSV model with (curve 3) set I and (curve 4) set II.

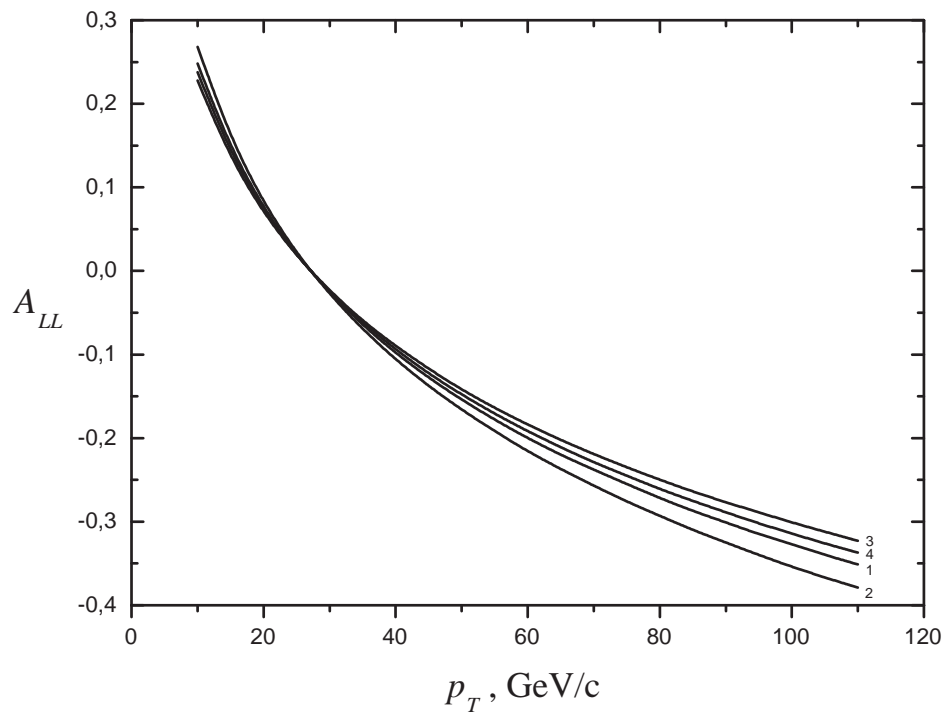


Figure 6: As in Fig.5, but for $Q = 60$ GeV.

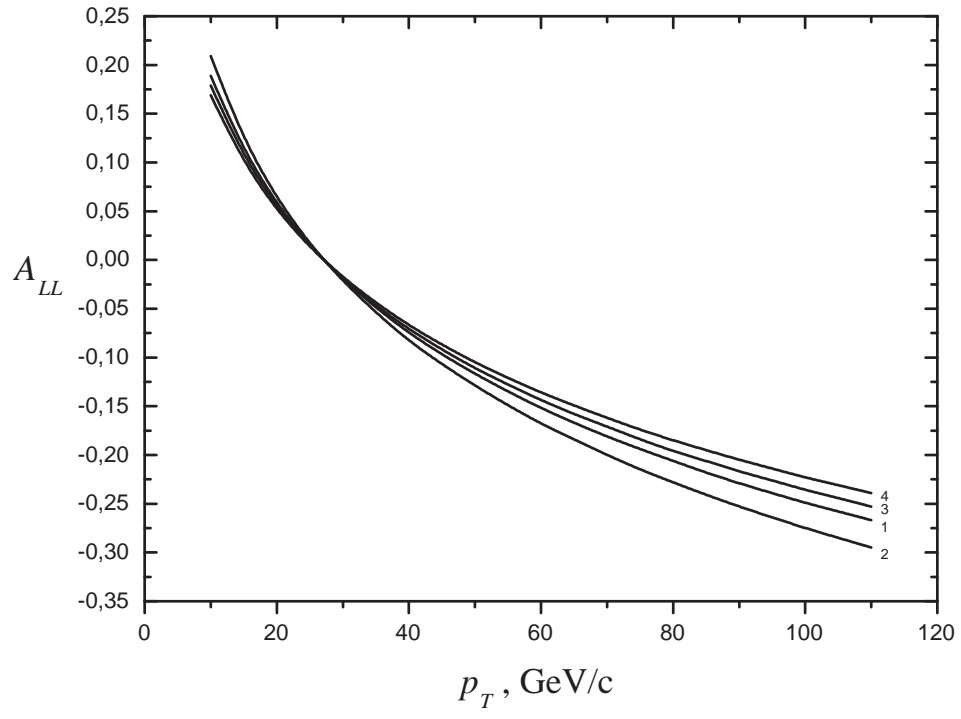


Figure 7: As in Fig.5, but for $Q = m_{Z^0}$.

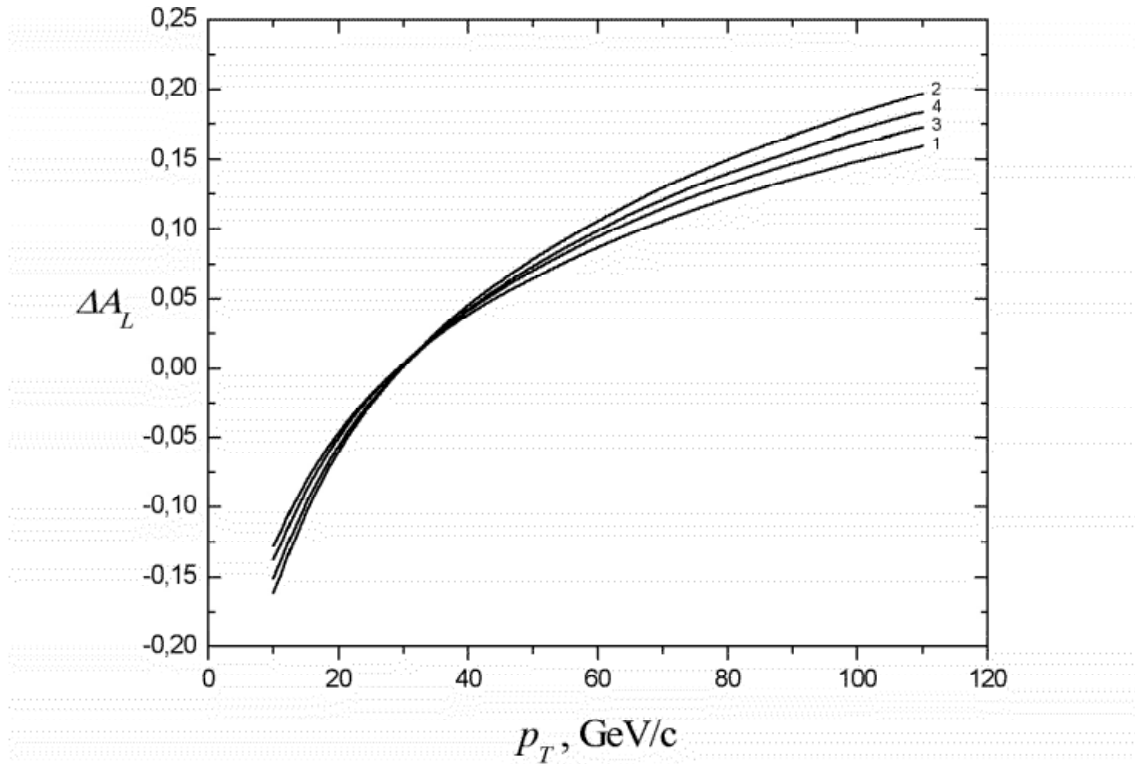


Figure 8: The dependence contribution Z' boson on the single-spin asymmetries ΔA_L as the function of the dilepton transverse momentum at $\sqrt{s} = 500$ GeV, the dilepton invariant mass of $Q = m_{Z^0}$, and the rapidity of $y = 0$. Shown are the asymmetries obtained on the basis of the CLW model with set I (curve 1) and set II (curve 2) and on the GRSW model with set I (curve 3) and set II (curve 4).

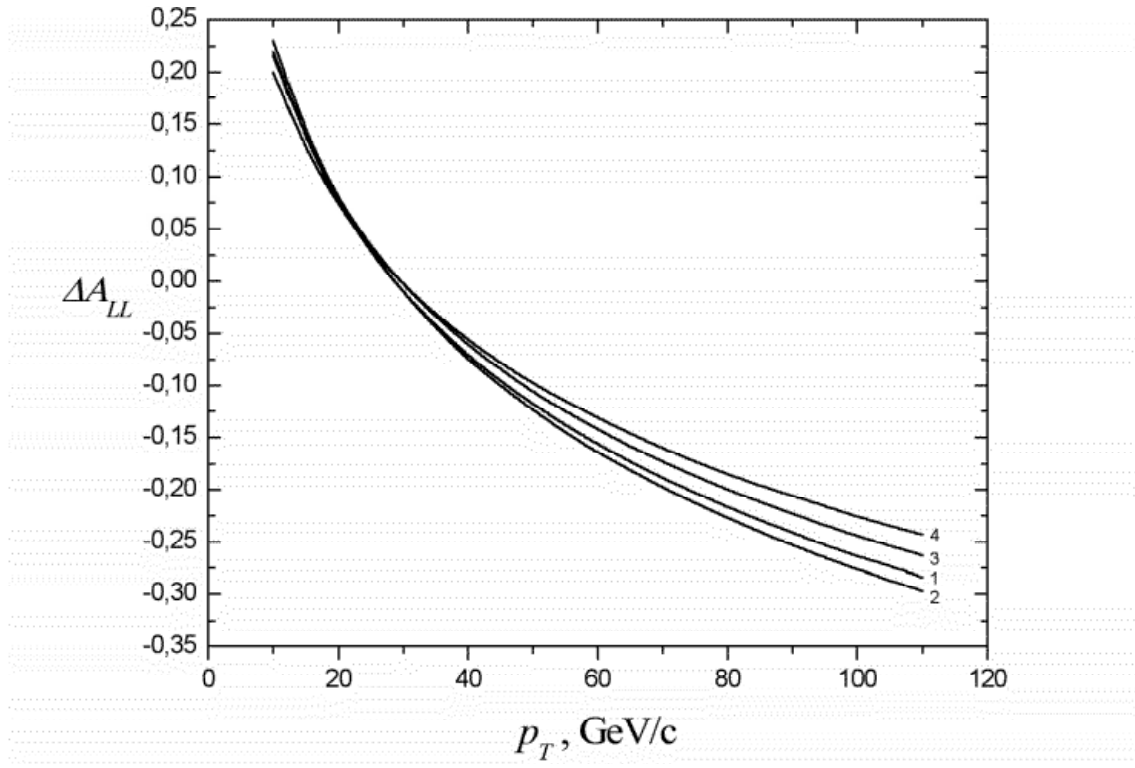


Figure 9: The dependence contribution Z' boson on the double-spin asymmetries ΔA_{LL} as the function of the dilepton transverse momentum at $\sqrt{s} = 500$ GeV, the dilepton invariant mass of $Q = 10$ GeV, and the rapidity of $y = 0$. Shown are the asymmetries obtained on the basis of the CLW model with set I (curve 1) and set II (curve 2) and on the GRSW model with set I (curve 3) and set II (curve 4).